

# Star Formation in Nearby Galaxies: The Role of *Webb*

Daniela Calzetti, [calzetti@astro.umass.edu](mailto:calzetti@astro.umass.edu), Jennifer E. Andrews, [jandrews@astro.umass.edu](mailto:jandrews@astro.umass.edu), & Alison F. Crocker, [alison.crocker@utoledo.edu](mailto:alison.crocker@utoledo.edu)

The hallmark high angular resolution and infrared capabilities of the *James Webb Space Telescope* will usher in a new epoch for studies of star formation in nearby galaxies. Decades of observations in the infrared and at other wavelengths, using both space- and ground-based facilities, have vastly increased our understanding of how star formation evolves in galaxies, and how it is related to a galaxy's general characteristics. Nevertheless, key questions remain unanswered. These include but are not limited to: (1) the physical link between local (molecular-cloud-level) and global (galaxy-scale) star formation; (2) the origin of the stellar Initial Mass Function (IMF); (3) the nature of correlation between central black holes and the host galaxy's bulge mass; and (4) the formation and evolution of dust, which is often used to trace star formation itself.

Answers to these questions can only come from *Webb* in combination with existing facilities offering high angular resolution, like *Hubble* and the Atacama Large Millimeter Array (ALMA). Those answers will provide the interpretative foundation for two of *Webb's* core science goals: understanding the history of galaxy assembly, from the early phases of the universe to the present day, and studying the light from the first stars and galaxies.

## Schmidt-Kennicutt Law

In the past several years, the connection between star formation and the gas supply in galaxies has been revealed by uniform surveys of nearby galaxies using a variety of telescopes: *Spitzer Space Telescope* and the *Herschel Space Observatory* in the infrared; *Galaxy Evolution Explorer* in the ultraviolet (UV); ground-based optical telescopes for nebular line emission; and H I and CO lines using ground-based radio and millimeter facilities. While the infrared, UV, and optical observations are used as diagnostics of current star-formation rate (SFR), the observations of H I and CO are tracers of atomic and molecular gas, respectively.

The now-standard formulation for connecting the SFR to the gas supply, also known as the Schmidt-Kennicutt Law (SK Law; Kennicutt 1998, Kennicutt & Evans 2012) is expressed as:

$$\Sigma_{\text{SFR}} = A (\Sigma_{\text{gas}})^{\gamma}$$

where  $\Sigma_{\text{SFR}}$  is the SFR surface density of a galaxy,  $\Sigma_{\text{gas}}$  its gas surface density,  $A$  is a scaling constant (i.e. the star formation efficiency if  $\gamma=1$ ), and  $\gamma$  is an exponent expected to be in the range  $\sim 1-2$ , and includes most of the physical information. The SK Law has been tested in many different environments and galaxies (Figure 1). So far, the results have been contradictory and non-conclusive; they disagree on whether such a relation is universal, what its physical underpinnings might be, and whether the law holds on all spatial scales, from individual molecular clouds to whole galaxies. The contradictions stem from the generally non-intersecting samples and the diverse observational strategies employed by studies on different scales. The dust-enshrouded early stages of star formation, which are the most closely related to the natal gas cloud and are traced via the emission from young stellar objects (YSOs), have been studied only in the Milky Way and its closest companions, the Magellanic Clouds. The reason is the limited angular resolution—2 arcsec or worse—of the infrared facilities that have been available so far (e.g., Shimonishi et al. 2010; Heiderman et al. 2010; Gutermuth et al. 2011; Sewilo et al. 2013).

With its sub-arcsecond capability in the mid-infrared, *Webb* will resolve individual YSOs in galaxies up to  $\sim 10$  times the distance of the Magellanic Clouds, or about 0.5–1 Mpc. The integrated light of dust-enshrouded star

formation in regions the size of molecular clouds ( $\sim 15-40$  pc) will be measured up to distances of  $\sim 10$  Mpc. To gain a quantitative appreciation of how large a volume *Webb* will probe, consider that today we can only study up to about 1 Mpc—roughly the distance of M33—with the same spatial resolution. This small volume contains only two massive galaxies (M33 and M31) in addition to the

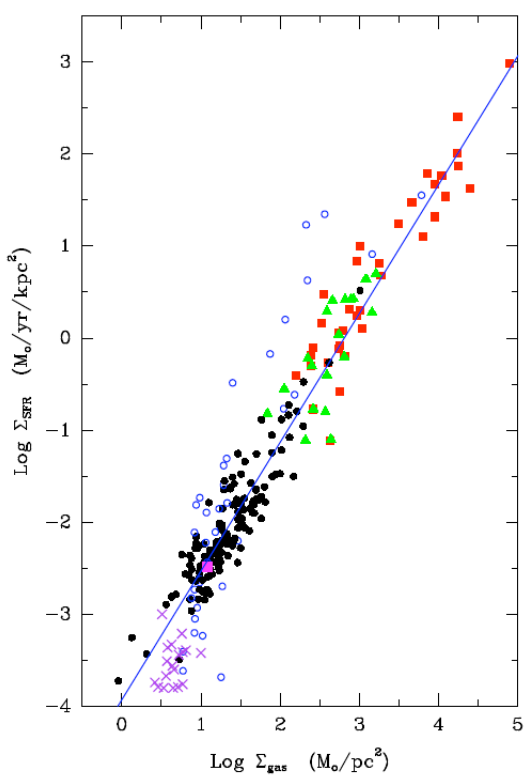


**Figure 1:** The relation in galaxies between the surface density of the star-formation rate surface density,  $\Sigma_{\text{SFR}}$ , and gas (atomic plus molecular) surface density,  $\Sigma_{\text{gas}}$ . Each data point is one galaxy. Black symbols are normal spiral and irregular galaxies; red squares are infrared-bright galaxies; green triangles are circumnuclear starbursts; purple crosses are galaxies with low surface brightness; blue circles are irregular and starburst galaxies with low metallicity and low mass. The magenta square is the Milky Way. The blue line has slope  $\gamma = 1.4$ . (From Figure 11 of Kennicutt & Evans 2012; reproduced with permission from the authors.)



Milky Way. However, massive galaxies are where most of the star formation takes place, and they are some of the key test beds for investigating the SK Law. Within the local  $\sim 10$  Mpc, 85% of the total SFR is contained in the  $\sim 80$  galaxies more massive than the Large Magellanic Cloud, and only 15% is contained in the remaining  $\sim 400$  galaxies.

The powerful combination of *Webb*, tracing dust-enshrouded star formation, and ALMA, tracing the molecular gas, will provide stepping stones on multiple fronts: (a) quantifying the duration of the dust-enshrouded phase of star formation and its dependence on local and global galactic conditions; (b) a solution to the diffuse/clustered star-formation dichotomy, whether it is an actual, physical separation or whether it is artificial, with star formation proceeding on a continuum of clustering scales; (c) the dependence of star-formation efficiency (the rate at which gas is converted into stars) on the local physical parameters; (d) an understanding of potential mediating mechanisms (e.g., stellar feedback; Hopkins et al. 2013) on the SFR–gas relation that separates different regimes and scales; and (e) ultimately, the physical underpinning of the SK Law as a function of spatial scale, from the molecular clouds within galaxies to the global galaxy population. Point (e) is fundamental for developing predictive theories of galaxy formation and evolution.

### Stellar IMF

The variety of conditions under which stars form in gas clouds provides an uneasy basis for a “universal” stellar IMF, meaning invariant as a function of location and time. Much debate still surrounds the stellar IMF, including whether or not it is universal (see Bastian et al. 2010; for a recent review). Theories of star formation lack the predictive power to inform observations, due to the intrinsically complex physics involved. As a result, both universal and variable IMFs are supported by models (e.g., Krumholz et al. 2010; Shadmehri & Elmegreen 2011). In the now-widely used formulations of the IMF by Kroupa (2001) and Chabrier (2003), 44% of the mass is contained in the 89% of stars with mass below  $1 M_{\odot}$ .

As a rule-of-thumb, any quantity related to SFRs, short-timescale ( $< 500$  Myr) star-formation histories, feedback, or chemical enrichment of galaxies, will involve the high-end of the IMF. This is because stars above a few solar masses emit, via stellar winds and supernovae explosions, virtually 100% of the ionizing photons, over 80% of the non-ionizing UV photons, and provide the vast majority of the energy, momentum, and chemical output from stars.

Conversely, the low-end of the IMF impacts the masses of galaxies and traces their star-formation histories on long timescales, as the low-mass stars—below  $0.9\text{--}1 M_{\odot}$ —accumulate throughout the Hubble time. Variations both at the high and low end of the IMF can have a major influence on the interpretation of galaxy evolution, as they affect measurements of galaxy masses and SFRs, for example, by factors 2 to 5, depending on the strength of the variation and the range of stellar masses considered. This impact can, additionally, be non-uniform across galaxy populations.

Direct measurements of the IMF, both at the low and high end, are available only for limited and less-crowded environments in the Milky Way and the Magellanic Clouds (Bastian et al. 2010). The same is true for a few low-density, faint galaxies near the Milky Way (e.g., Geha et al. 2013; using *Hubble*). The latter finding tentatively indicates a systematic variation at the low end of the IMF with galactic environment (Figure 2).

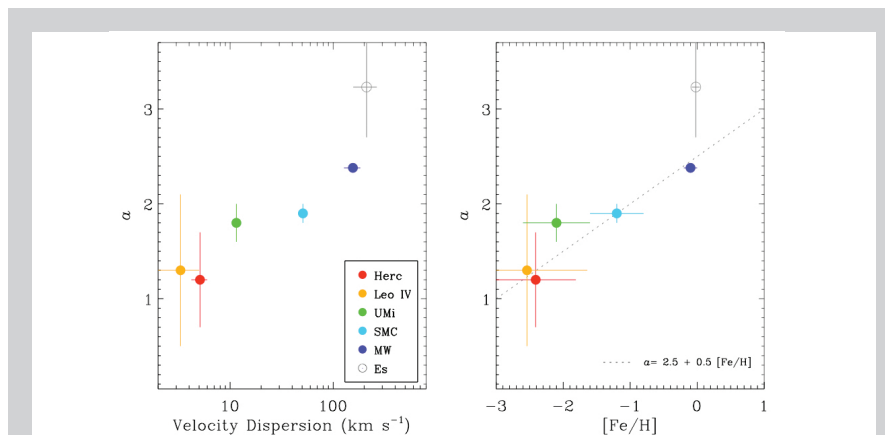


**Figure 2:** Variations in the power law slope  $\alpha$  (where  $dN/dm \sim m^{-\alpha}$ ) of the low end of the stellar IMF, in the mass range  $\sim 0.5\text{--}0.8 M_{\odot}$ , as determined from direct star counts in a handful of nearby ( $< 40$  kpc) galaxies and the Milky Way (color circles). The indirect measure for elliptical galaxies is shown as the empty black circle. The slope is plotted as a function of the velocity dispersion (*left panel*) and the metal abundance (*right panel*) of the galaxy. In the *right panel*, the dotted line is from a model suggested by Kroupa (2001). (From Figure 5 of Geha et al. 2013; reproduced with permission from the authors.)

Far more abundant are the indirect measures of the IMF, using integrated light from galaxies. At the high end of the IMF, results are controversial (compare Andrews et al. 2013 with Lee et al. 2009 and Meurer et al. 2009), owing to the degeneracies involved, mainly between IMF and the star-formation history. Conversely, the mass-to-light ratios of elliptical galaxies (e.g., Cappellari et al. 2012) indicate variations for the low end of the IMF consistent with the results of Geha et al. (2013). Far from settled, these results are still tentative, and, in the case of the direct measures, based on small-number statistics.

*Webb* will be key for addressing the low end of the IMF through direct measures. Star counts in the near-IR will be possible in a  $\sim 500$  times larger volume than is currently possible with *Hubble*. The observations will extend out to the virial radius of the Milky Way ( $\sim 300$  kpc), improving the statistics more than five-fold from the current handful of galaxies to  $>25$ , (Geha 2014). These observations will produce tight constraints on IMF theories (Offner et al. 2013).

### **Black holes & bulge velocity dispersion**

There is a tight relation between black-hole mass and the velocity dispersion of the bulge, which related to the bulge mass (e.g., Gültekin et al. 2009). This tightness suggests the presence of a regulating mechanism in the growth of black holes that efficiently couples with the bulge's stellar properties. Any coupling, however, must be effective over a significant range of spatial scales, from a black hole's accretion disk ( $< \sim 0.1$  pc) to a bulge (several kpc). This spatial range corresponds to a range of timescales. One scenario suggests the existence of multiple black-hole feedback mechanisms that cause gas removal from the black hole's surroundings, effectively quenching star formation. When coupled with ineffective cooling, these mechanisms provide a channel for black-hole self-regulation (Hopkins et al. 2009; Roth et al. 2012). Another scenario prescribes a connection between black holes and bulge mass via gas stabilization in pressure-supported bulges (Martig et al. 2009). This "morphological quenching" predicts an overall low efficiency of star formation in early-type galaxies. Current observations cannot uniquely resolve the tension between "normal" and "reduced" star-formation efficiency in the central regions of early-type galaxies, owing to the contamination of star-formation tracers by the emission from active galactic nuclei (AGNs) in low-resolution infrared data (Crocker et al. 2012; Martig et al. 2013). This will be prime territory for the *Webb*: the integral field unit in the Mid-Infrared Instrument will be able to identify the key line diagnostics for star formation and AGN gas excitation—and to separate the emission from the two components—at unprecedented resolution in the local early-type galaxies in the iconic surveys (e.g., ATLAS3D; Cappellari et al. 2011). In combination with ALMA, *Webb* will determine the efficiency of star formation in these systems, and establish whether reduced star-formation efficiencies are tied to the relation between the mass of black holes and the velocity dispersion in the bulge.

### **Dust emission**

The dust emission from galaxies, and from star-forming regions within galaxies, is used as a tracer of dust-enshrouded star formation at all redshifts. The spectral range shortward of the peak of the infrared emission, including thermal and non-thermal continuum and the emission features of the polycyclic aromatic hydrocarbons (PAHs), has been calibrated as a SFR indicator in a number of papers, using data from a variety of space facilities (e.g., Calzetti et al. 2007, 2010; Kennicutt et al. 2009; Rieke et al. 2009; Liu et al. 2011). Longward of the infrared peak, the strongest correlations are found with the dust and cold-gas content of galaxies. Despite the global-scale proportionality between infrared emission and SFR, important deviations are observed when looking closely at the galaxies. For instance, significant fractions of the emission in the Wien tail of the dust thermal continuum ( $\sim 20$ – $30$  microns), and in the region of the PAH emission features ( $\sim 8$  microns), have been found to be due to dust heated by old stellar populations, rather than by young, star-forming regions. These fractions vary from galaxy to galaxy, but are generally around 30%–60% for the thermal continuum of the dust, and about 40%–80% for the PAH features (e.g., Verley et al. 2009; Crocker et al. 2013; Calapa et al. 2014). Equally important is the fact that the PAH emission features—some of the key SFR tracers for high-redshift galaxy populations—are depressed both in low-metallicity environments (Engelbracht et al. 2005, 2008; Draine et al. 2007; Smith et al. 2007) and within regions of active star formation (e.g., Helou et al. 2004; Bendo et al. 2008; Relano & Kennicutt 2009). This is possibly an effect of dust processing (Madden et al. 2006; Gordon et al. 2008). One detailed study of the Small Magellanic Cloud at spatial scales of  $< 1$  pc finds that the PAH emission is both depressed in H<sub>II</sub> regions, confirming previous findings, and enhanced in molecular clouds (Sandstrom et al. 2010). Overall, we still have poor constraints on the life cycle of the dust components within galaxies, mainly because detailed studies have been limited to the cases of the Milky Way and the Magellanic Clouds, with only lower-resolution analyses in more distant galaxies.

Understanding dust formation is as important as understanding the processing of dust. Dust production in core-collapse supernovae (CCSNe) is an open question that has fundamental implications for interpreting high-redshift galaxies. Dust masses as large as  $10^8 M_{\odot}$  are observed in the host galaxies of quasi-stellar objects at  $z \sim 6.5$ , when the universe is  $< 800$  Myr old (Bertoldi et al. 2003). Such large dust masses require a fast and efficient channel of dust production. The short-lived CCSNe are

candidates for quickly returning material back to the interstellar medium. In the local universe, however, dust yields from CCSNe have been measured to be generally a few orders of magnitude less than the  $0.1\text{--}1 M_{\odot}$  per CCSN needed to account for the dust masses observed in high-redshift galaxies (e.g., Nozawa et al. 2003; Cherchneff & Dwek 2010). Only recently, ALMA observations of SN 1987A in the Large Magellanic Cloud (Indebetouw et al. 2014) have revealed that at least  $0.2 M_{\odot}$  of cool dust has formed in the inner ejecta. Nevertheless, it is still unclear what fraction of that dust will survive. These studies are still hampered by small-number statistics, together with the difficulty of separating intervening dust from the dust produced by the SN itself.

*Webb's* mid-infrared imaging and spectroscopic capabilities will extend analyses of dust emission at spatial scales of  $1\text{--}10$  pc to a volume of space 1,000 times larger than that probed so far, extending all the way to 10 Mpc distance and probing the full range of global and local-galaxy properties. The investigation of dust formation in CCSNe will be extended to distances well beyond 10 Mpc, with detailed analyses of the mid-IR spectral diagnostics that trace newly formed dust and its composition. This increased diversity of galaxies will enable the study of the mechanisms that form and process the different dust components across all galactic environments, and over the spatial scales of star-forming regions, gas clouds, and supernova remnants. Understanding the life cycles of the different dust components under varying conditions will provide the physical grounding for extrapolating the locally calibrated dust-enshrouded SFRs to the conditions of the early universe, and for pinning down the nature of the dust at high redshift.

In summary, *Webb's* capabilities will provide answers to fundamental open questions on the physical processes that govern star formation in galaxies. Nearby galaxies offer the best locales for exploring these processes at the spatial scales relevant for star formation itself, namely those of star-forming regions and gas clouds. The answers to those questions will provide the foundation for transforming measurements of distant galaxies into physical quantities, and interpreting those quantities within the framework offered by theoretical models of galaxy evolution.

#### References:

- Andrews, J. E., Calzetti, D., Chandar, R., et al. 2013, ApJ, 767, 51  
Bastian, N., Covey, K. R., & Meyer, M. R. 2010, ARAA, 48, 339  
Bendo, G. J., Draine, B. T., Engelbracht, C. W., et al. 2008, MNRAS, 389, 629  
Bertoldi, F., Carilli, C. L., Cox, P., et al. 2003, A&A, 406, L55  
Calapa, M., Calzetti, D., Draine, B. T., et al. 2014, ApJ, submitted  
Calzetti, D., Kennicutt, R. C., Engelbracht, C. W. et al. 2007, ApJ, 666, 870  
Calzetti, D., Wu, S.-Y., Hong, S., et al. 2010, ApJ, 714, 1256  
Cappellari, M., Emsellem, E., Krajnovic, D., et al. 2011, MNRAS, 413, 813  
Cappellari, M., McDermid, R. M., Alatalo, K., et al. 2012, Anture, 484, 485  
Chabrier, G. 2003, PASP, 115, 763  
Cherchneff, I., & Dwek, E. 2010, ApJ, 713, 1  
Crocker, A. F., Calzetti, D., Thilker, D., et al. 2013, ApJ, 762, 79  
Crocker, A. F., Krips, M., Bureau, M., et al. 2012, MNRAS, 421, 1298  
Draine, B. T., Dale, D. A., Bendo, G. et al. 2007, ApJ, 633, 866  
Engelbracht, C. W., Gordon, K. D., Rieke, G. H., et al. 2005, ApJ, 628, 29  
Engelbracht, C. W., Rieke, G. H., Gordon, K. D., et al. 2008, ApJ, 685, 678  
Geha, M. C. 2014, BAAS, 223, 314.03  
Geha, M. C., Brown, T. M., Tumlinson, J., et al. 2013, ApJ, 771, 29  
Gordon, K. D., Engelbracht, C. W., Rieke, G. H., et al. 2008, ApJ, 682, 336  
Gültekin, K., Richstone, D. O., Gebhardt, K., et al. 2009, ApJ, 698, 198  
Gutermuth, R. A., Pipher, J. L., Megeath, S. T., et al. 2011, ApJ, 739, 84  
Heiderman, A., Evans, N., Allen, L. E., et al. 2010, ApJ, 723, 1019  
Helou, G., Roussel, H., Appleton, P., et al. 2004, ApJS, 154, 253  
Hopkins, P. F., Murray, N., & Thomson, T. A. 2009, MNRAS, 398, 303  
Hopkins, P. F., Narayanan, D., & Murray, N. 2013, MNRAS, 432, 2647  
Indebetouw, R., Matsuura, M., Dwek, E., et al. 2014, ApJ, 782, L2  
Kennicutt, R. C. 1998, ApJ, 498, 541  
Kennicutt, R. C., & Evans, N. J. 2012, ARAA, 50, 531  
Kennicutt, R. C., Hao, C., Calzetti, D., et al. 2009, ApJ, 703, 1672  
Kroupa, P. 2001, MNRAS, 322, 231  
Krumholz, M. R., Cunningham, A. J., Klein, R. I., & McKee, C. F. 2010, ApJ, 713, 1120  
Lee, J. C., Gil de Paz, A., Tremonti, C., et al. 2009, ApJ, 706, 599  
Liu, G., Koda, J., Calzetti, D., et al. 2011, ApJ, 735, 63  
Madden, S. C., Galliano, F., Jones, A. P., & Sauvage, M. 2006, A&A, 446, 877  
Martig, M., Bournaud, F., Teyssier, R., & Dekel, A. 2009, ApJ, 714, L275

Martig, M., Crocker, A. F., Bournaud, F., et al. 2013, MNRAS, 432, 1914  
Meurer, G. R., Wong, O. I., Kim, J. H., et al. 2009, ApJ, 695, 765  
Nozawa, T., Kozasa, T., Umeda, H., et al. 2003, ApJ, 598, 785  
Offner, S. R., Clark, P. C., Hennebelle, P., et al. 2013, in *Protostars and Planets VI*, University of Arizona Press (2014), eds. H. Beuther, R. S. Klessen, C. P. Dullemond, and Th. Henning  
Relano, M., & Kennicutt, R. C. 2009, ApJ, 699, 1125  
Rieke, G. H., Alonso-Herrero, A., Weiner, B. J., et al. 2009, ApJ, 692, 556  
Roth, N., Kasen, D., Hopkins, P. F., & Quataert, E. 2012, ApJ, 759, 36  
Sandstrom, K. M., Bolatto, A. D., Draine, B. T., et al. 2010, ApJ, 715, 701  
Sewilo, M., Carlson, L. R., Seale, J. P., et al. 2013, ApJ, 778, 15  
Shadmehri, M., & Emegreen, B. G., 2011, MNRAS, 410, 788  
Shimonishi, T., Onaka, T., Kato, D., et al. 2010, A&A, 514, A12  
Smith, J. D. T., Draine, B. T., Dale, D. A., et al. 2007, ApJ, 656, 770  
Verley, S., Corbelli, E., Giovanardi, C., & Hunt, L. K. 2009, A&A, 493, 453